

PAPER • OPEN ACCESS

## $\Lambda_c^+$ physics at BESIII

To cite this article: Weiping Wang and BESIII collaboration 2018 *J. Phys.: Conf. Ser.* **1024** 012034

View the [article online](#) for updates and enhancements.

### Related content

- [Recent results, status and prospects for the BESIII experiment](#)  
Isabella Garzia and BESIII Collaboration
- [Light Hadron Spectroscopy at BESIII](#)  
Jifeng Hu and BESIII Collaboration
- [Modelling Hadronic Matter](#)  
Débora P. Menezes

# $\Lambda_c^+$ physics at BESIII

**Weiping Wang (on behalf of the BESIII collaboration)**

University of Science and Technology of China, No.96, JinZhai Road Baohe District, Hefei, Anhui, 230026, P.R.China.

E-mail: cloud13@mail.ustc.edu.cn

**Abstract.** Based on the data sets collected by the BESIII detector near the  $\Lambda_c^+ \bar{\Lambda}_c^-$  production threshold, *i.e.* at  $\sqrt{s} = 4574.5, 4580.0, 4590.0,$  and  $4599.5$  MeV, we report the preliminary study of the production behaviour of  $e^+e^- \rightarrow \Lambda_c^+ \bar{\Lambda}_c^-$  process, including the Born cross section and electromagnetic form factor ratios. Using the large statistic data at  $\sqrt{s} = 4599.5$  MeV, we measured the absolute branching fractions of Cabibbo-favored hadronic decays of  $\Lambda_c^+$  baryon with a double-tag technique. The branching fractions for 12 hadronic decay modes are significantly improved. We also report the model-independent measurement of the branching fraction of  $\Lambda_c^+ \rightarrow \Lambda e^+ \nu_e$  and  $\Lambda_c^+ \rightarrow \Lambda \mu^+ \nu_\mu$  semi-leptonic decays.

## 1. Introduction

The electromagnetic structure of hadrons, parameterized in terms of electromagnetic form factors (EMFFs) provides a key to understand the strong interaction. Assuming that one-photon exchange dominates the production of spin 1/2 baryons  $B$ , the Born cross section of the process  $e^+e^- \rightarrow B\bar{B}$  can be parameterized in terms of EMFFs, *i.e.*  $G_E$  and  $G_M$ , in the following way [1]:

$$\sigma_{B\bar{B}}(s) = \frac{4\pi\alpha^2 C\beta}{3s} |G_M(s)|^2 \left[ 1 + \frac{2m_B^2 c^4}{s} \left| \frac{G_E(s)}{G_M(s)} \right|^2 \right]. \quad (1)$$

Here  $\alpha$  is the fine-structure constant  $\beta = \sqrt{1 - 4m_B^2 c^4/s}$  the velocity of the baryon,  $s$  the square of center-of-mass (CM) energy and  $m_B$  is the mass of the baryon. The Coulomb factor  $C$  parameterizes the electromagnetic interaction between the outgoing baryon-antibaryon pair. For neutral baryons the Coulomb factor is equal to 1, while for point-like charged fermions it is equal to  $C = \varepsilon R$  [2, 3], where  $\varepsilon = \pi\alpha/\beta$  is an enhancement factor resulting in a nonzero cross section at threshold, and  $R = \sqrt{1 - \beta^2}/(1 - e^{-\pi\alpha/\beta})$  is the Sommerfeld resummation factor. In the  $e^+e^- \rightarrow p\bar{p}$  process, the BaBar collaboration observed a rapid rise of the cross section near threshold, followed by a plateau around 200 MeV above threshold [4]. The BESIII collaboration also observed the cross section enhancement [5]. The non-vanishing cross section near threshold as well as the wide-range plateau have led to various theoretical interpretations [6, 7, 8]. Recently, the BESIII collaboration has observed the non-zero cross section near threshold in the  $e^+e^- \rightarrow \Lambda\bar{\Lambda}$  process. Naturally, it is also interesting to explore the production behaviour of  $\Lambda_c^+$ , the lightest baryon containing the charm quark. Previously, the Belle collaboration measured the cross section of  $e^+e^- \rightarrow \Lambda_c^+ \bar{\Lambda}_c^-$  using initial-state radiation (ISR) technique [9], but the results suffer from significant uncertainties in CM energy and cross section. Therefore, near  $\Lambda_c^+ \bar{\Lambda}_c^-$  threshold, precise measurements of the production Born cross section and EMFF ratios are highly needed.



The decays of charm baryon provide crucial information for the study of both strong and weak interactions. The hadronic decays of  $\Lambda_c^+$  provide important input to  $\Lambda_b$  physics, while the semi-leptonic (SL) decays of  $\Lambda_c^+$  provide a stringent test on non-perturbative theoretical models. The  $\Lambda_c^+ \rightarrow \Lambda l^+ \nu_l$  decay is dominated by the Cabibbo-favored transition  $c \rightarrow sl^+ \nu_l$ , which occurs, to a good approximation, independently on the spin-zero spectator  $ud$  di-quark. In addition, theoretical calculations are proved to be quite challenging for lattice quantum chromodynamics (LQCD) due to the complexity of form factors in  $\Lambda_c^+ \rightarrow \Lambda l^+ \nu_l$  [10]. Consequently, the model-independent measurement of hadronic and SL decays with better precision is a key ingredient in theoretical predictions and LQCD calculation, which in turn will play an important role in understanding different  $\Lambda_c^+$  decays.

## 2. The production of $\Lambda_c^+$

The Born cross section of  $e^+e^- \rightarrow \Lambda_c^+ \bar{\Lambda}_c^-$  reaction is measured at four CM energies:  $\sqrt{s} = 4574.5, 4580.0, 4590.0,$  and  $4599.5$  MeV. At each CM energy, 10 Cabibbo-favored hadronic decay modes:  $\Lambda_c^+ \rightarrow pK^-\pi^+, pK_S^0, \Lambda\pi^+, pK^-\pi^+\pi^0, pK_S^0\pi^0, \Lambda\pi^+\pi^0, pK_S^0\pi^+\pi^-, \Lambda\pi^+\pi^+\pi^-, \Sigma^0\pi^+,$  and  $\Sigma^+\pi^+\pi^-$ , as well as the 10 corresponding charge-conjugate modes, are independently reconstructed. Each mode will produce one measurement of the Born cross section, and the total cross section is obtained from weighted average over the 20 individual measurements [11]. The resulting cross sections at four CM energies are listed in Table 1 and shown in Figure 1 together with the Belle data [9] for comparison.

**Table 1.** The average Born cross section of  $e^+e^- \rightarrow \Lambda_c^+ \bar{\Lambda}_c^-$  measured at each CM energy, where the uncertainties are statistical and systematic, respectively (BESIII preliminary results). The  $\mathcal{L}_{\text{int}}$  denotes the integrated luminosity, and the  $f_{\text{ISR}}$  represents for the ISR correction factor.

$\sqrt{s}$ (MeV)	$\mathcal{L}_{\text{int}}$ ( $\text{pb}^{-1}$ )	$f_{\text{ISR}}$	$\sigma$ (pb)
4574.5	47.67	0.45	$236 \pm 11 \pm 46$
4580.0	8.54	0.66	$207 \pm 17 \pm 13$
4590.0	8.16	0.71	$245 \pm 19 \pm 16$
4599.5	566.93	0.74	$237 \pm 3 \pm 15$

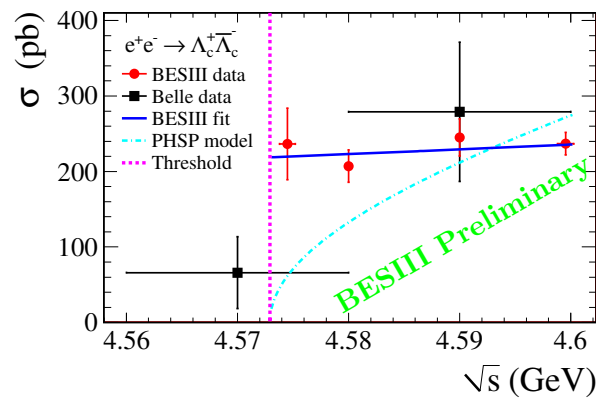


**Figure 1.** The Born cross section of  $e^+e^- \rightarrow \Lambda_c^+ \bar{\Lambda}_c^-$  obtained by BESIII (this work) and Belle. The blue solid curve represents the input line-shape for KKMC, the Monte Carlo (MC) generator inside the BESIII framework, when determining the  $f_{\text{ISR}}$ . The dash-dot cyan curve denotes the prediction of the phase space (PHSP) model.

The data collected at  $\sqrt{s} = 4574.5$  and  $4599.5$  MeV are large enough to perform a detailed study in the CM frame of the  $\Lambda_c$  polar angle  $\theta_{\Lambda_c}$ , which is defined as the angle between the  $\Lambda_c$  momentum and the beam direction. The data fulfilling all selection criteria are divided into 10 bins in  $\cos\theta_{\Lambda_c}$ . In each  $\cos\theta_{\Lambda_c}$  bin, the total yield is obtained by summing yields of all the 10 tagged modes. The one-dimensional bin-by-bin efficiency corrections are applied to these total yields. The same procedure is performed by tagging  $\bar{\Lambda}_c^-$  decay channels. The total yields of  $\Lambda_c^+$  and  $\bar{\Lambda}_c^-$  are combined bin-by-bin, and the shape function  $f(\theta) \propto (1 + \alpha_{\Lambda_c} \cos^2\theta)$  is fitted to the combined data, as shown in Figure 2.

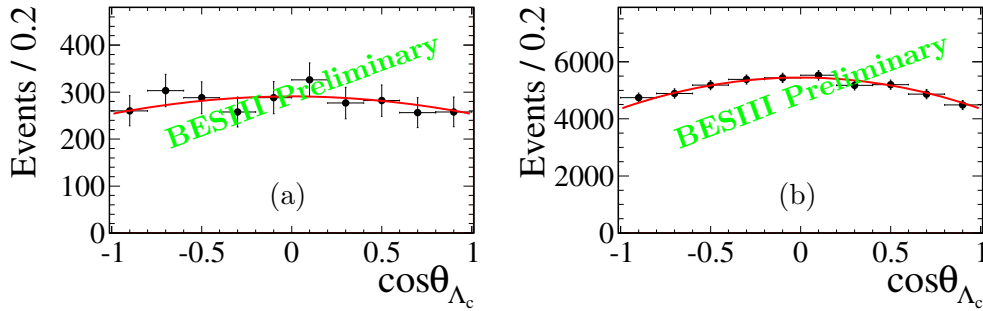


**Figure 2.** The angular distribution and corresponding fit results in data at  $\sqrt{s} = 4574.5$  MeV (a) and  $4599.5$  MeV (b).

Table 2 lists the resulting  $\alpha_{\Lambda_c}$  parameters obtained from the fits, as well as the  $|G_E/G_M|$  ratios extracted using the equation:

$$|G_E/G_M|^2(1 - \beta^2) = (1 - \alpha_{\Lambda_c})/(1 + \alpha_{\Lambda_c}). \quad (2)$$

**Table 2.** Shape parameters of the angular distribution and  $|G_E/G_M|$  ratios at  $\sqrt{s} = 4574.5$  and  $4599.5$  MeV. The uncertainties are statistical and systematic (BESIII preliminary results).

$\sqrt{s}$ (MeV)	$\alpha_{\Lambda_c}$	$ G_E/G_M $
4574.5	$-0.13 \pm 0.12 \pm 0.08$	$1.14 \pm 0.14 \pm 0.07$
4599.5	$-0.20 \pm 0.04 \pm 0.02$	$1.23 \pm 0.05 \pm 0.03$

### 3. $\Lambda_c^+$ hadronic decay

Based on the data sample with an integrated luminosity of  $566.9 \text{ pb}^{-1}$  collected with the BESIII detector [12] at  $\sqrt{s} = 4599.5$  MeV, we apply a tagged technique pioneered by the MARK-III Collaboration [13] to determine the branching fraction (BF) of  $\Lambda_c^+$  hadronic decay. To identify the  $\Lambda_c^+\bar{\Lambda}_c^-$  signal candidates, we firstly reconstruct one  $\bar{\Lambda}_c^-$  baryon [called single tag (ST)] through the final states of any of the singly tagged modes. For a given decay mode  $j$ , the ST yields is

$$N_j^{\text{ST}} = N_{\Lambda_c^+\bar{\Lambda}_c^-} \cdot \mathcal{B}_j \cdot \varepsilon_j, \quad (3)$$

where  $N_{\Lambda_c^+\bar{\Lambda}_c^-}$  is the total number of produced  $\Lambda_c^+\bar{\Lambda}_c^-$  pairs, and  $\varepsilon_j$  is the corresponding efficiency. Then we define double-tag (DT) events as those where the partner  $\Lambda_c^+$  recoiling against the  $\bar{\Lambda}_c^-$  is reconstructed in one of the signal modes. That is, in DT events, both the  $\Lambda_c^+$  and  $\bar{\Lambda}_c^-$  are reconstructed. The DT yield with  $\Lambda_c^+ \rightarrow i$  (signal mode) and  $\bar{\Lambda}_c^- \rightarrow j$  (tagging mode) is

$$N_{ij}^{\text{DT}} = N_{\Lambda_c^+\bar{\Lambda}_c^-} \cdot \mathcal{B}_i \cdot \mathcal{B}_j \cdot \varepsilon_{ij}, \quad (4)$$

**Table 3.** Comparison of the measured BFs in this work [14] with previous results from PDG [15]. For our results, the first uncertainties are statistical and the second are systematic.

Mode	This work (%)	PDG (%)
$pK_S^0$	$1.52 \pm 0.08 \pm 0.03$	$1.15 \pm 0.30$
$pK^- \pi^+$	$5.84 \pm 0.27 \pm 0.23$	$5.0 \pm 1.3$
$pK_S^0 \pi^0$	$1.87 \pm 0.13 \pm 0.05$	$1.65 \pm 0.50$
$pK_S^0 \pi^+ \pi^-$	$1.53 \pm 0.11 \pm 0.09$	$1.30 \pm 0.35$
$pK^- \pi^+ \pi^0$	$4.53 \pm 0.23 \pm 0.30$	$3.4 \pm 1.0$
$\Lambda \pi^+$	$1.24 \pm 0.07 \pm 0.03$	$1.07 \pm 0.28$
$\Lambda \pi^+ \pi^0$	$7.01 \pm 0.37 \pm 0.19$	$3.6 \pm 1.3$
$\Lambda \pi^+ \pi^- \pi^+$	$3.81 \pm 0.24 \pm 0.18$	$2.6 \pm 0.7$
$\Sigma^0 \pi^+$	$1.27 \pm 0.08 \pm 0.03$	$1.05 \pm 0.28$
$\Sigma^+ \pi^0$	$1.18 \pm 0.10 \pm 0.03$	$1.00 \pm 0.34$
$\Sigma^+ \pi^+ \pi^-$	$4.25 \pm 0.24 \pm 0.20$	$3.6 \pm 1.0$
$\Sigma^+ \omega$	$1.56 \pm 0.20 \pm 0.07$	$2.7 \pm 1.0$

where  $\varepsilon_{ij}$  is the efficiency for simultaneously reconstructing modes  $i$  and  $j$ . Hence, the ratio of the DT yield ( $N_{ij}^{\text{DT}}$ ) and ST yield ( $N_j^{\text{ST}}$ ) provides an absolute measurement of the BF:

$$\mathcal{B}_i = \frac{N_{ij}^{\text{DT}} \varepsilon_j}{N_j^{\text{ST}} \varepsilon_{ij}}. \quad (5)$$

Because of the large acceptance of the BESIII detector and the low multiplicities of  $\Lambda_c$  hadronic decays,  $\varepsilon_{ij} \approx \varepsilon_i \varepsilon_j$ . Hence, the ratio  $\varepsilon_j / \varepsilon_{ij}$  is insensitive to most systematic effects associated with the decay mode  $j$ , and a signal BF  $\mathcal{B}_i$  obtained using this procedure is nearly independent on the efficiency of the tagging mode. Therefore  $\mathcal{B}_i$  is sensitive to the signal mode efficiency ( $\varepsilon_i$ ), whose uncertainties dominate the contribution to the systematic error from the efficiencies. We use a least-squares fitter, which considers statistical and systematic correlations among the different hadronic modes, to obtain the BFs of the 12  $\Lambda_c^+$  decay modes globally. In total, there are 13 free parameters (12  $\mathcal{B}_i$  and 1  $N_{\Lambda_c^+ \bar{\Lambda}_c^-}$ ) to be estimated. The extracted BFs of  $\Lambda_c^+$  are listed in Table 3. The total number of  $\Lambda_c^+ \bar{\Lambda}_c^-$  pairs produced is obtained to be  $N_{\Lambda_c^+ \bar{\Lambda}_c^-} = (105.9 \pm 4.8 \pm 0.5) \times 10^3$ . The goodness of fit is evaluated as  $\chi^2 / \text{ndf} = 9.9 / (24 - 13) = 0.9$ .

#### 4. $\Lambda_c^+$ semi-leptonic decay

Using the similar strategy in hadronic decay measurements, we select the data sample of  $\bar{\Lambda}_c^-$  baryons by reconstructing exclusive hadronic decays. The ST  $\bar{\Lambda}_c^-$  are reconstructed using 11 hadronic decay modes:  $\bar{\Lambda}_c^- \rightarrow \bar{p}K_S^0$ ,  $\bar{p}K^+ \pi^-$ ,  $\bar{p}K_S^0 \pi^0$ ,  $\bar{p}K^+ \pi^- \pi^0$ ,  $\bar{p}K_S^0 \pi^+ \pi^-$ ,  $\bar{\Lambda} \pi^-$ ,  $\bar{\Lambda} \pi^- \pi^0$ ,  $\bar{\Lambda} \pi^- \pi^+ \pi^-$ ,  $\bar{\Sigma}^0 \pi^-$ ,  $\bar{\Sigma}^- \pi^0$  and  $\bar{\Sigma}^- \pi^+ \pi^-$ , where the intermediate particles  $K_S^0$ ,  $\bar{\Lambda}$ ,  $\bar{\Sigma}^0$ ,  $\bar{\Sigma}^-$  and  $\pi^0$  are reconstructed by their decays into  $K_S^0 \rightarrow \pi^+ \pi^-$ ,  $\bar{\Lambda} \rightarrow \bar{p} \pi^+$ ,  $\bar{\Sigma}^0 \rightarrow \gamma \bar{\Lambda}$  and  $\bar{\Lambda} \rightarrow \bar{p} \pi^+$ ,  $\bar{\Sigma}^- \rightarrow \bar{p} \pi^0$  and  $\pi^0 \rightarrow \gamma \gamma$ , respectively. The total observed events for the 11 ST modes is  $N_{\Lambda_c^+ \text{tag}} = (14415 \pm 159)$ . The signal candidates for  $\Lambda_c^+ \rightarrow \Lambda^+ \nu_l$  are selected from the remaining tracks recoiling against the ST  $\bar{\Lambda}_c^-$  candidates. As the neutrino is the missing particle of the event, we employ a variable

$$U_{\text{miss}} = E_{\text{miss}} - c|\vec{p}_{\text{miss}}|$$

to obtain information of the neutrino, where  $E_{\text{miss}}$  and  $\vec{p}_{\text{miss}}$  are the missing energy and momentum carried by the neutrino, respectively. They are calculated by  $E_{\text{miss}} = E_{\text{beam}} -$

$E_\Lambda - E_{e^+}$ , and  $\vec{p}_{\text{miss}} = \vec{p}_{\Lambda_c^+} - \vec{p}_\Lambda - \vec{p}_{e^+}$ , where  $\vec{p}_{\Lambda_c^+}$  is the momentum of  $\Lambda_c^+$  baryon,  $E_\Lambda(\vec{p}_\Lambda)$  and  $E_{e^+}(\vec{p}_{e^+})$  are the energies (momenta) of the  $\Lambda$  and the positron, respectively. Here, the  $\vec{p}_{\Lambda_c^+}$  is given by  $\vec{p}_{\Lambda_c^+} = -\hat{p}_{\text{tag}}\sqrt{E_{\text{beam}}^2 - m_{\Lambda_c^-}^2}$ , where  $\hat{p}_{\text{tag}}$  is the momentum direction of ST  $\bar{\Lambda}_c^-$  and  $m_{\Lambda_c^-}$  is the nominal  $\bar{\Lambda}_c^-$  mass. For signal events,  $U_{\text{miss}}$  is expected to peak around zero.

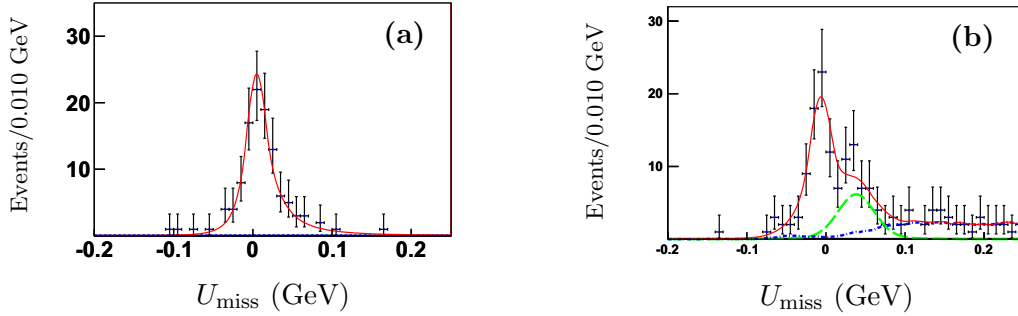


**Figure 3.** (a) Fit to the  $U_{\text{miss}}$  distribution of process  $\Lambda_c^+ \rightarrow \Lambda e^+ \nu_e$  [16]. (b) Fit to the  $U_{\text{miss}}$  distribution of process  $\Lambda_c^+ \rightarrow \Lambda \mu^+ \nu_\mu$  [17]. The points with error bars are data, the (red) solid curve shows the total fit and the (blue) dashed curve is the background shape. The green-dashed line in the right subfigure denotes the MC-driven background shapes which is supposed to simulate the remaining background.

Figure 3(a) shows the fit result of the  $U_{\text{miss}}$  distribution for  $\Lambda_c^+ \rightarrow \Lambda e^+ \nu_e$ . From the fit, we obtain the number of SL signals to be  $(109.4 \pm 10.9)$ . After subtracting all the background, we determine the net number of  $\Lambda_c^+ \rightarrow \Lambda e^+ \nu_e$  to be  $N_{\text{semi}} = (103.5 \pm 10.9)$ , where the uncertainty is statistical. The absolute BF for  $\Lambda_c^+ \rightarrow \Lambda e^+ \nu_e$  is determined by

$$\mathcal{B}(\Lambda_c^+ \rightarrow \Lambda e^+ \nu_e) = \frac{N_{\text{semi}}}{N_{\Lambda_c^-}^{\text{tot}} \times \varepsilon_{\text{semi}} \times \mathcal{B}(\Lambda \rightarrow p \pi^-)}, \quad (6)$$

where  $\varepsilon_{\text{semi}} = (30.92 \pm 0.26)\%$  is the overall efficiency for detecting the  $\Lambda_c^+ \rightarrow \Lambda e^+ \nu_e$  decay in ST events, weighted by the ST yields of data for each tag. Inserting the values of  $N_{\text{semi}}$ ,  $N_{\Lambda_c^-}^{\text{tot}}$ ,  $\varepsilon_{\text{semi}}$  and  $\mathcal{B}(\Lambda \rightarrow p \pi^-)$  in Eq. (6), we get  $\mathcal{B}(\Lambda_c^+ \rightarrow \Lambda e^+ \nu_e) = (3.63 \pm 0.38 \pm 0.20)\%$ , where the first error is statistical and the second systematic.

Using an analogous technique to that of  $\Lambda_c^+ \rightarrow \Lambda e^+ \nu_e$ , in which the  $U_{\text{miss}}$  is used as the final signal variable, the process  $\Lambda_c^+ \rightarrow \Lambda \mu^+ \nu_\mu$  is also studied. The fitting model includes MC-driven background shapes to simulate the remaining background, shown in Fig. 3(b). Accordingly, the  $\mathcal{B}(\Lambda_c^+ \rightarrow \Lambda \mu^+ \nu_\mu)$  is determined to be  $(3.49 \pm 0.46 \pm 0.27)\%$ . With the result of  $\mathcal{B}(\Lambda_c^+ \rightarrow \Lambda e^+ \nu_e)$  in hand, the ratio  $\mathcal{B}(\Lambda_c^+ \rightarrow \Lambda e^+ \nu_e)/\mathcal{B}(\Lambda_c^+ \rightarrow \Lambda \mu^+ \nu_\mu)$  is obtained to be  $(0.96 \pm 0.16(\text{stat.}) \pm 0.04(\text{sys.}))\%$ , which verified the lepton universality in baryon decays.

## 5. Summary

In summary, based on the data sets collected by BESIII detector near the  $\Lambda_c^+ \bar{\Lambda}_c^-$  production threshold, we report the preliminary study of the production behaviour of  $e^+ e^- \rightarrow \Lambda_c^+ \bar{\Lambda}_c^-$  process, including the Born cross section and electromagnetic form factor ratios. Using the data at  $\sqrt{s} = 4599.5$  MeV, BESIII performed the first measurement of the absolute hadronic branching fractions of 12 Cabibbo-favored decays of  $\Lambda_c^+$ . BESIII also presented the first model-independent measurement of the branching fractions of the semi-leptonic decay  $\Lambda_c^+ \rightarrow \Lambda e^+ \nu_e$  and  $\Lambda_c^+ \rightarrow \Lambda \mu^+ \nu_\mu$ .

## 6. Reference

- [1] Cabibbo N and Gatto R, *Phys. Rev.* **124** 1577
- [2] Sommerfeld A, *Ann. Phys.* **403** 257
- [3] Sakharov A D, *Sov. Phys. Usp.* **34** 375
- [4] Lees J P *et al.* (BaBar Collaboration), *Phys. Rev. D* **87** 092005; Lees J P *et al.* (BaBar Collaboration), *Phys. Rev. D* **88** 072009
- [5] Ablikim M *et al.* (BESIII Collaboration), *Phys. Rev. D* **91** 112004
- [6] Dalkarov O D, Khakhulin P A and Voronin A Yu, *Nucl. Phys. A* **833** 104
- [7] El-Bennich B, Lacombe M, Loiseau B and Wycech S, *Phys. Rev. C* **79** 054001; Haidenbauer J, Hammer H W, Messener U G and Sibirtsev A, *Phys. Lett. B* **643** 29
- [8] Baldini R, Pacetti S, Zallo A and Zichichi A, *Eur. Phys. J. A* **39** 315; Baldini R, Pacetti S and Zallo A, *Eur. Phys. J. A* **48** 33
- [9] Pakhlova G *et al.* (Belle Collaboration), *Phys. Rev. Lett.* **101** 172001
- [10] Rosner J L, *Phys. Rev. D* **86** 014017
- [11] Schmelling M, *Phys. Scripta* **51** 676
- [12] Ablikim M *et al.* (BESIII Collaboration), *Nucl. Instrum. Meth. A* **614** 345
- [13] Baltrusaitis R M *et al.* (MARK-III Collaboration), *Phys. Rev. Lett.* **56** 2140; Adler J *et al.* (MARK-III Collaboration), *Phys. Rev. Lett.* **60** 89
- [14] Ablikim M *et al.* (BESIII Collaboration), *Phys. Rev. Lett.* **116** 052001
- [15] Olive K A *et al.* (Particle Data Group), *Chin. Phys. C* **38** 090001
- [16] Ablikim M *et al.* (BESIII Collaboration), *Phys. Rev. Lett.* **115** 221805
- [17] Ablikim M *et al.* (BESIII Collaboration), *Phys. Lett. B* **767** 42